



Research report

Coherent neocortical gamma oscillations decrease during REM sleep in the rat



Matías Cavelli^a, Santiago Castro^a, Natalia Schwarzkopf^a, Michael H. Chase^{b,c},
Atilio Falconi^a, Pablo Torterolo^{a,*}

^a Laboratorio de Neurobiología del Sueño, Departamento de Fisiología, Facultad de Medicina, Universidad de la República, General Flores 2125, 11800 Montevideo, Uruguay

^b WebSciences International, 1251 Westwood Blvd., Los Angeles, CA 90024, USA

^c UCLA School of Medicine, Los Angeles, CA 90095, USA

HIGHLIGHTS

- The electroencephalogram of adult rats was recorded during sleep and wakefulness.
- The intra and inter-hemispheric coherence of the EEG gamma band was analyzed.
- The coherence was larger in W and almost absent during REM sleep.

ARTICLE INFO

Article history:

Received 8 October 2014

Received in revised form

19 December 2014

Accepted 23 December 2014

Available online 31 December 2014

Keywords:

Cortex

Consciousness

EEG

Synchronization

Coherence

ABSTRACT

Higher cognitive functions require the integration and coordination of large populations of neurons in cortical and subcortical regions. Oscillations in the high frequency band (30–100 Hz) of the electroencephalogram (EEG), that have been postulated to be a product of this interaction, are involved in the binding of spatially separated but temporally correlated neural events, which results in a unified perceptual experience. The extent of this functional connectivity can be examined by means of the mathematical algorithm called “coherence”, which is correlated with the “strength” of functional interactions between cortical areas. As a continuation of previous studies in the cat [6,7], the present study was conducted to analyze EEG coherence in the gamma band of the rat during wakefulness (W), non-REM (NREM) sleep and REM sleep.

Rats were implanted with electrodes in different cortical areas to record EEG activity, and the magnitude squared coherence values within the gamma frequency band of EEG (30–48 and 52–100 Hz) were determined.

Coherence between all cortical regions in the low and high gamma frequency bands was greater during W compared with sleep. Remarkably, EEG coherence in the low and high gamma bands was smallest during REM sleep.

We conclude that high frequency interactions between cortical areas are radically different during sleep and wakefulness in the rat. Since this feature is conserved in other mammals, including humans, we suggest that the uncoupling of gamma frequency activity during REM sleep is a defining trait of REM sleep in mammals.

© 2015 Elsevier B.V. All rights reserved.

1. Introduction

Electroencephalographic (EEG) oscillations in the gamma frequency (30–100 Hz) band are involved in the integration or

binding of spatially separated but temporally correlated neural events [1–3]. An increase in gamma power typically appears during states/behaviors that are characterized by the active cognitive processing of external percepts or internally generated thoughts and images in humans and during alert wakefulness in animals [4–7].

The degree of EEG coherence between two cortical regions is correlated with the strength of the functional interconnections

* Corresponding author. Tel.: +598 2924 34 14x3234.
E-mail address: ptorterolo@fmed.edu.uy (P. Torterolo).

that occur between them [1,2,8,9]. Recently, Siegel et al. (2012) have proposed that frequency-specific correlated oscillations in distributed cortical networks provide indices, or ‘fingerprints’, of the network interactions that underlie cognitive processes [10].

Gamma coherence between different brain areas, which is greatest during wakefulness (W) has been viewed as a possible neural correlate of consciousness [11]. In effect, coherence in the gamma frequency band decreases during narcosis (unconsciousness) induced by anesthesia [12,13].

During deep non-REM (NREM) sleep there is an absence, or at least a strong reduction in cognitive functions. In contrast, dreams that occur more prominently during rapid eye movement (REM) sleep, are considered a special kind of cognitive activity or proto-consciousness [14]. Recently, we demonstrated in the cat that there is high level of neocortical intra and interhemispheric gamma coherence during alert wakefulness, it decreases during quiet W and NREM sleep, and is almost absent during REM sleep [6,7].

In the present report, we evaluated the extent of EEG 30–100 Hz coherence between intra and interhemispheric neocortical activity during naturally occurring sleep and W in the rat.

2. Materials and methods

2.1. Experimental animals

Twelve adult male Wistar rats (300–350 g) were used in this study. The animals were determined to be in good health by the Institutional Animal Care Facility. All of the animals were maintained on a 12:12-h light-dark cycle under controlled temperature (21–24 °C) conditions with free access to food and water. All of the experimental procedures were conducted in accord with the *Guide for the Care and Use of Laboratory Animals* (8th edition, National Academy Press, Washington, DC, 2010) and approved by the Institutional Animal Care Commission (protocol No. 071140-001931-12, Facultad de Medicina, Universidad de la República). Adequate measures were taken to minimize pain, discomfort or stress of the animals. In addition, all efforts were made in order to use the minimal number of animals necessary to produce reliable scientific data.

2.2. Surgical procedures

The surgical procedures employed were similar to those in our previous studies [15,16]. The animals were chronically implanted with electrodes to monitor the states of sleep and W. Anesthesia was induced with a mixture of ketamine-xylazine (90 mg/kg; 5 mg/kg i.p. respectively). The animal's head was positioned in a stereotaxic frame and the skull was exposed. In order to record the EEG, stainless steel screw electrodes were placed in the calvarium, overlying the parietal and occipital cortices and the cerebellum (Fig. 1). Bipolar electrodes were inserted into the neck muscle in order to record the electromyogram (EMG). The electrodes were connected to a plug that was bonded to the skull with acrylic cement.

At the end of the surgical procedures, an analgesic was administered. Incision margins were kept clean and a topical antibiotic was administered on a daily basis. After the animals had recovered from the preceding surgical procedures, they were adapted to the recording environment for a period of at least one week.

2.3. Experimental sessions

Experimental sessions of 6 h in duration were conducted during the light period, between 12 A.M. and 6 P.M. in a temperature controlled (21–24 °C) and sound attenuated chamber. All animals had free access to water and food. During these sessions (as well

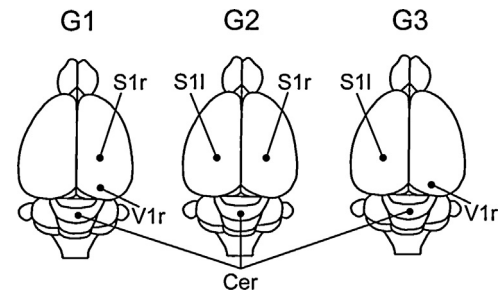


Fig. 1. Position of recording electrodes. The figure presents a summary of the position of the recording electrodes on the surface of the primary somatosensory and primary visual cortices (according to Ref. [31]). The electrodes were referred to a common electrode that was located over the cerebellum (Cer). G1–G3, are groups of animals with different electrode locations (four animals per group). S1, somatosensory primary cortex; V1, visual primary cortex; r, right; l, left.

as during the adaptation sessions), the animals were able to move freely within the confines of the recording-chamber.

EEG and EMG of each rat were recorded daily for a period of approximately 2 weeks in order to obtain a complete data set. The activity of two cortical areas was recorded simultaneously with monopolar electrodes. A common electrode reference montage was placed on the cerebellar surface; this montage is critical for the analysis of coherence [17–21]. For each pair of recordings, data were obtained during four recording sessions, and for every combination of electrodes, in three groups (G1–G3) of 4 rats (Fig. 1).

Bioelectric signals were amplified ($\times 1000$), filtered (0.1–200 Hz), sampled (512 Hz, 16 bits) and stored in a PC using Spike 2 software (Cambridge Electronic Design). Data were obtained during spontaneously occurring W, NREM and REM sleep. The presence of low voltage fast waves in the parietal cortex, a mixed theta rhythm (4–7 Hz) in the occipital cortex and relatively high electromyographic activity were used to identify W. Light and deep NREM sleep were determined, but only epochs of established periods of deep NREM sleep were utilized for coherence analysis. Deep NREM sleep was identified by the presence of continuous high amplitude slow (0.5–4 Hz) frontal and occipital waves and sleep spindles (9–15 Hz) combined with a reduced EMG activity. REM sleep was identified by the occurrence of low voltage fast parietal waves, a regular theta rhythm in the occipital cortex, and the absence of EMG activity except for occasional muscular twitches [15].

2.4. Data analysis

Sleep and waking states were determined in epochs of 10 s [15]. In order to obtain power spectral and coherence values between a pair of EEG channels, we used procedures that we have previously employed [6,7]. Artifacts were detected in the raw recording and in the spectrogram (with a 0.5 s resolution); artifacts produced a general increase in power and were usually associated with movements. Twelve independent artifact-free periods of 100 s were selected and examined during each behavioral state (1200 s for each behavioral state per rat).

For each 100 s period, the Magnitude Squared Coherence was determined as follows: $\text{coh}_{ab}(f) = [\sum \text{csd}_{ab}(f)]^2 / [\sum \text{psd}_a(f) \sum \text{psd}_b(f)]$, where psd is the power spectral density and a and b are the waves that are analyzed. csd is the cross spectra density, or the Fourier transform of the cross covariance function, which provides a statement of how common activity between two processes is distributed across frequencies. Coherence between two waveforms is a function of frequency and ranges from 0 for totally incoherent waveforms to 1 for maximal coherence. In order for two waveforms to be completely coherent at a particular frequency over a

given time range, the phase shift between the waveforms must be constant and the amplitudes of the waves must have a constant ratio.

We obtained power spectrum and the magnitude squared coherence using the Spike 2 script COHER 1S (Cambridge Electronic Design). By employing this method, we were able to analyze the coherence between two EEG channels that were recorded simultaneously during 100 s periods. This analysis period was divided into 100 time-blocks with a sampling rate of 512 Hz, a bin size of 1024 samples (512 for each channel) and a resolution of 0.5 Hz. Analyses of serial, non-overlapping, 10 s epochs were also used to determine the temporal dynamic of the coherence (Figs. 5 and 6).

We concentrated on examining the coherence of the EEG in the gamma frequency band (30–48 and 52–100 Hz); low and high gamma bands were also analyzed in our previous studies in cats, where they exhibited differences in relation to attentive behaviors

[6,7]. Fifty Hz electrical noise was also avoided with this partition. In order to eliminate the possibility that gamma activity and coherence were produced by extra-cerebral potentials, we performed the same procedures and analysis than in our previous studies (see [6,7] for details).

In order to normalize the data and evaluate them by means of parametric statistical tests, we applied the Fisher z' transform to the gamma coherence values. The z' -coherence of the gamma band for each pair of EEG channels was averaged across behavioral states. z' -Coherence was expressed as the mean \pm standard error. The significance of the differences among behavioral states, cortical sites and interactions were evaluated with two-ways ANOVA and Tukey tests. The z' -coherence across behavioral states for the intra or interhemispheric combination of electrodes was also evaluated by one-way ANOVA and Tamhane tests. The gamma power for the different cortices among behavioral states was also evaluated with

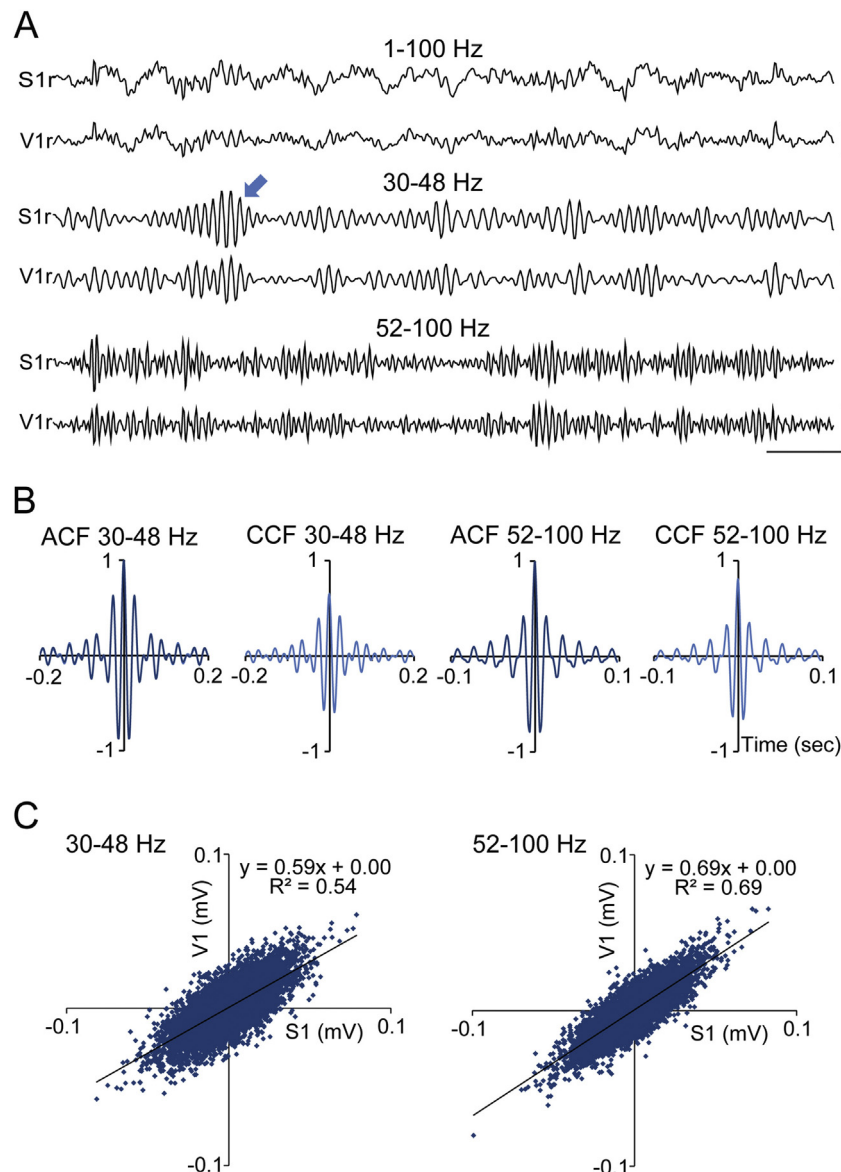


Fig. 2. Gamma oscillations during wakefulness. (A) Simultaneous raw and filtered (35–48 and 52–100 Hz) recordings from the right somatosensory primary (S1r) and right visual primary (V1r) cortices during wakefulness. Gamma oscillations, which are readily observed in the raw recordings, are highlighted after filtering. An arrow signals a “burst” of gamma oscillations. Calibration bars: 200 ms and 200 μ V for raw recordings and 100 μ V for filtered recordings. (B) Autocorrelation function (ACF) and cross-correlation functions (CCF) from filtered (35–48 Hz and 52–100 Hz) periods of 100 s of simultaneous EEG recordings from S1r and V1r are shown during W. The ACF of both channels are superimposed. (C) Linear regression between the amplitudes of S1r and V1r was performed on representative filtered recordings (30–48 and 52–100 Hz) during 20 s of wakefulness. The determination coefficients and regression line equations are shown.

one-way ANOVA and Tamhane tests. The criterion used to reject the null hypotheses was $p < 0.05$.

Selected recordings were filtered, with a band pass of 30–48 and 52–100 Hz, using Spike 2 digital finite impulse response filters. The amplitude of simultaneously recorded pairs of filtered EEG signals was also analyzed by means of the Pearson correlation. Autocorrelations and cross-correlations functions were also computed.

3. Results

3.1. Raw and filtered (30–48 and 52–100 Hz) EEG recordings during wakefulness and REM sleep

The EEG fluctuates between a desynchronized pattern of activity in the presence of theta rhythm during W and REM sleep and synchronized slow wave activity during NREM sleep. Although EEG

activity during W and REM sleep is similar, there are subtle differences. Representative EEG recordings during W and REM sleep are shown in Figs. 2 and 3, respectively. Oscillations of approximately 30–48 Hz can be observed in raw recordings during W (Fig. 2); these electrographic events are not clear during REM sleep (Fig. 3).

Gamma oscillations 30–48 or 52–100 Hz, were unmasked after digital filtering of the recordings. During W, gamma oscillations at 30–48 Hz exhibited some burst of activity with spindle morphology (see example in Fig. 2, arrow); on the other hand, 52–100 Hz oscillations were irregular without a clear pattern. In spite of this, the autocorrelation functions show the presence of an oscillatory pattern of gamma activity (for 30–48 and 52–100 Hz) both during W and REM (Figs. 2 and 3).

Fig. 2 also illustrates a representative example of the coupling of EEG signals recorded from different cortical sites of the same hemisphere during W. Coupling was highlighted when the amplitudes of the signals between pairs of simultaneous EEG recordings were

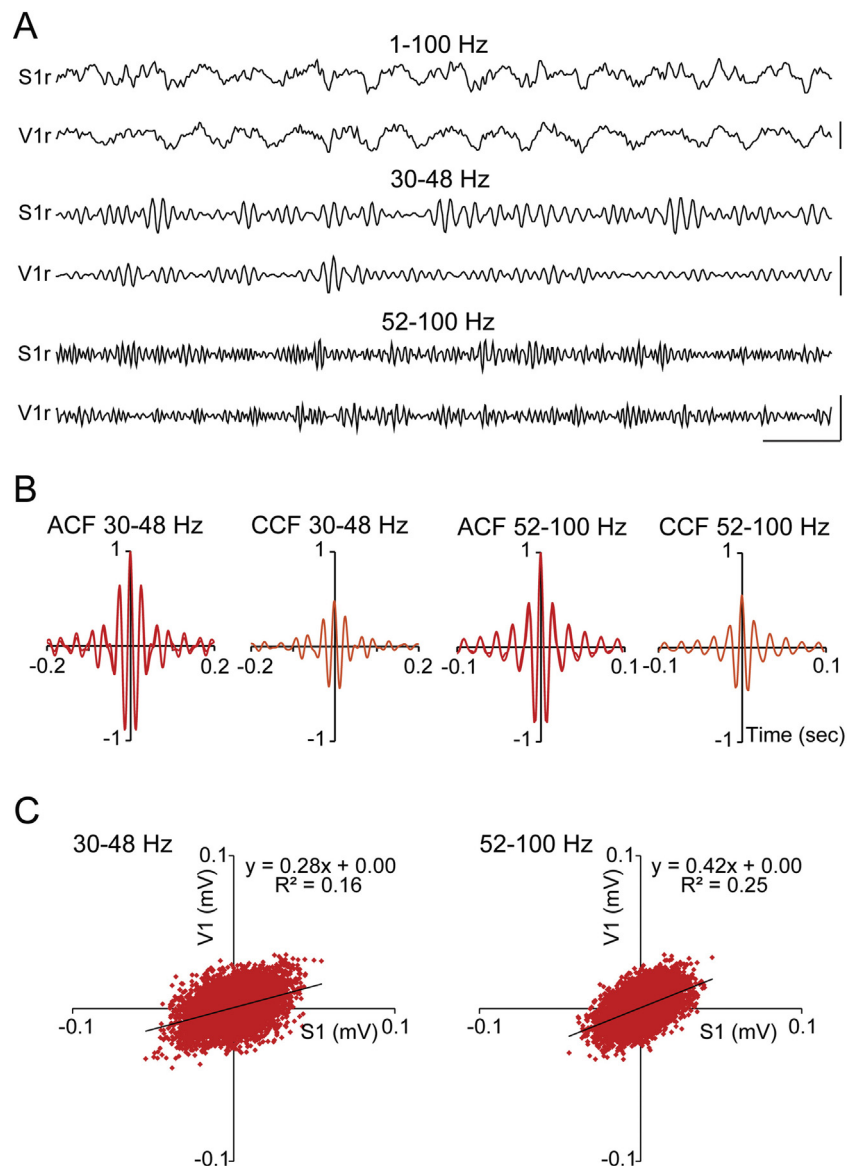


Fig. 3. Gamma oscillations during REM sleep. (A) Simultaneous raw and filtered (35–48 and 52–100 Hz) recordings from the right somatosensory primary (S1r) and right visual primary (V1r) cortices during REM sleep. The amplitude and duration of gamma oscillations decreased compared to wakefulness (see Fig. 2). Calibration bars: 200 ms and 200 μ V for raw recordings and 100 μ V for filtered recordings. (B) Autocorrelation (ACF) and cross-correlation functions (CCF) from filtered (35–48 Hz and 52–100 Hz) periods of 100 s of simultaneous EEG recordings from S1r and V1r are shown during REM sleep. The ACF of both channels are superimposed. (C) Linear regression between the amplitudes of S1r and V1r were analyzed from representative filtered recordings (30–48 and 52–100 Hz) during 20 s of REM sleep. The determination coefficients and regression line equations are shown.

correlated; the cross-correlation function also shows that both waves are strongly coupled. During REM sleep, the intrahemispheric EEG coupling is reduced, which can be observed in the filtered recordings, the correlation and the cross-correlation histogram exhibited in Fig. 3.

3.2. Coherent 30–48 and 52–100 Hz activity is reduced during REM sleep

In addition to the fact that EEG coupling was minimal during REM sleep when analyzed by filtered recordings and correlation methods, we utilized the magnitude-squared coherence for an in-depth analysis of different pairs of EEG signals that were simultaneously recorded during W and sleep.

As a first step, by means of the two-ways ANOVA we analyzed z' -coherence using behavioral states, and intra- or interhemispheric combination of electrodes (derivates) as factors. The analyses revealed a significant effect of behavioral states (30–48 Hz, $F_{2,423} = 47.28$, $p < 0.0001$; 52–100 Hz, $F_{2,423} = 232.2$, $p < 0.0001$), derivates (30–48 Hz, $F_{2,423} = 335.5$, $p < 0.0001$; 52–100 Hz, $F_{2,423} = 242.4$, $p < 0.0001$) and interactions (30–48 Hz, $F_{4,423} = 8.508$, $p < 0.0001$; 52–100 Hz, $F_{4,423} = 4.497$, $p = 0.001$). Tukey *post hoc* analyses showed that, disregarding the derivates, 30–48 Hz z' -coherence during REM sleep was different than during the other behavioral states ($p < 0.001$). In addition, disregarding behavioral states, 30–48 Hz z' -coherence in the heterotopic interhemispheric combination was different than in the others derivates ($p < 0.001$). All of the combination (behavioral states and derivates) were statistically significant ($p < 0.001$) for 52–100 Hz z' -coherence.

As a second step, we analyzed the z' -coherence in each combination of electrodes across behavioral states using one-way ANOVA. There were significant differences for the intrahemispheric (30–48 Hz, $F_{2,141} = 27.81$, $p < 0.0001$; 52–100 Hz, $F_{2,141} = 94.39$, $p < 0.0001$); the interhemispheric homotopic (30–48 Hz, $F_{2,141} = 8.501$, $p < 0.0001$; 52–100 Hz, $F_{2,141} = 58.95$, $p < 0.0001$) and interhemispheric heterotopic derivates (30–48 Hz, $F_{2,141} = 32.52$, $p < 0.0001$; 52–100 Hz, $F_{2,141} = 95.68$, $p < 0.0001$).

In Fig. 4 is readily observed that, for all the derivates, the minimum values of the z' -coherence for both 30–48 and 52–100 Hz were during REM sleep. For the 30–48 Hz band, in the intrahemispheric derivates, maximum values were present during W. In interhemispheric heterotopic combination, the maximum value of z' -coherence was during NREM sleep. The z' -coherence for 52–100 Hz band was significantly greater during W both for intra and interhemispheric derivates (Fig. 4). The schematic presented in Fig. 4B summarizes the gamma z' -coherence during W and sleep.

For an in-depth analysis of the transitions (t) into and from REM sleep, we analyzed the mean gamma z' -coherence during t (Fig. 5). REM sleep onset was accompanied by a decrease in z' -coherence that was maintained at a low level during this state (Fig. 5A). In contrast, during the transition from REM sleep either to W or NREM sleep, z' -coherence increased (Fig. 5B).

An example of the dynamic evolution of EEG coherence in gamma (30–48 and 52–100 Hz) across behavioral states is shown in Fig. 6 for the intrahemispheric combination of electrodes. While the maximal values of z' -coherence were present during W, the minimal values occurred during REM sleep episodes (Fig. 6).

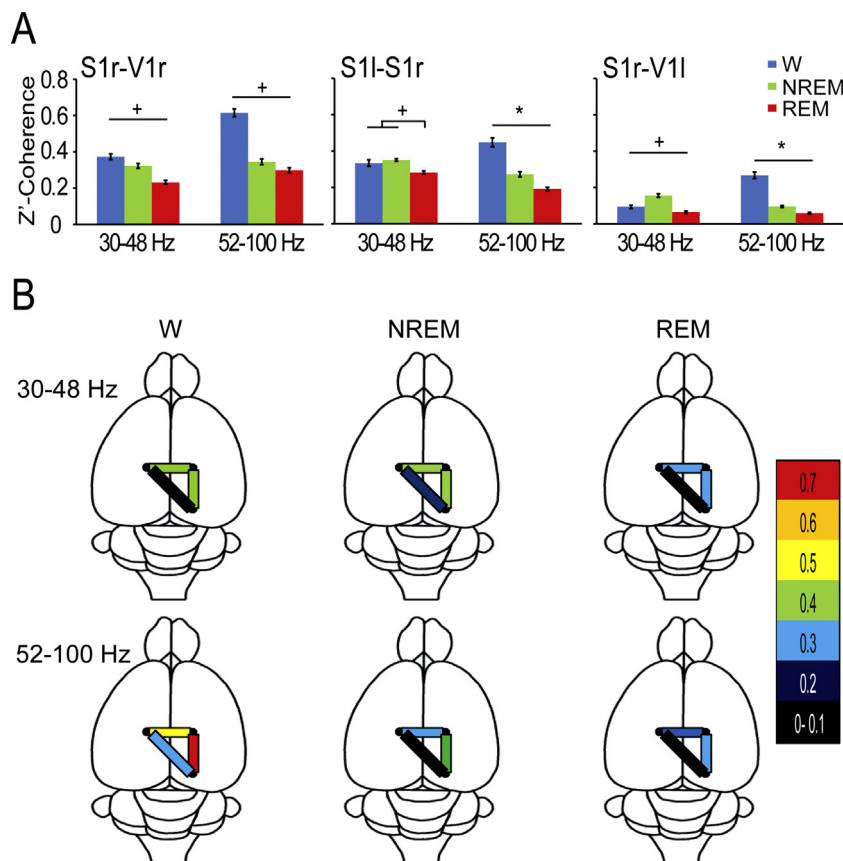


Fig. 4. Gamma band z' -coherence during wakefulness and sleep. (A) Mean z' -coherence (30–48 and 52–100 Hz) of intrahemispheric (G1, S1r–V1r), interhemispheric homotopic (G2, S1l–S1r) and interhemispheric heterotopic (G3, S1r–V1l) combination of electrodes. Data were obtained from 4 rats per group; 12 windows of 100 s per rat for each behavioral state. The values represent the mean \pm standard error. Statistical significance: * $p < 0.05$ and * $p < 0.0001$; ANOVA and Tamhane tests. (B) Summary of the gamma band EEG z' -coherence. The lines represent derivates and the color represents the level of z' -coherence. (For interpretation of the references to color in this figure legend, the reader is referred to the web version of this article.)

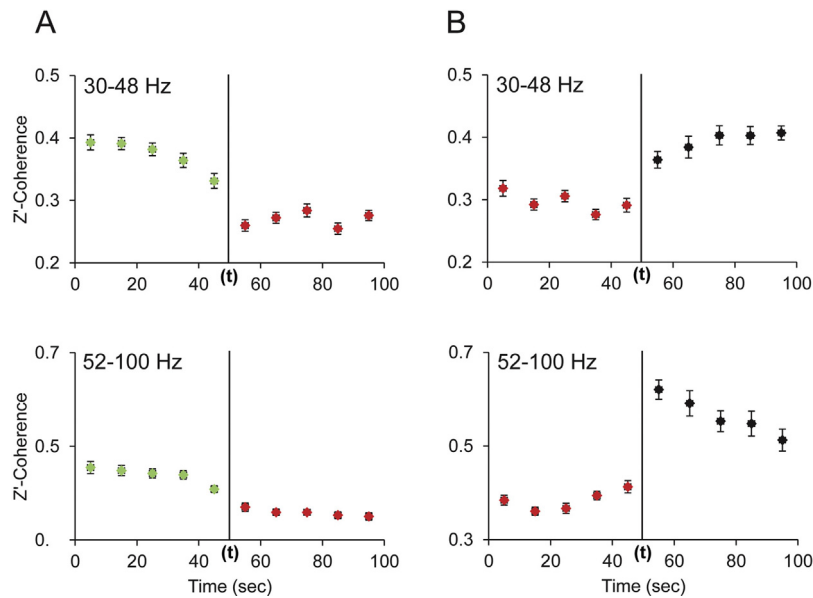


Fig. 5. z' -Coherence during REM sleep transitions. (A) The graphs depict the mean z' -coherence \pm standard error (for 30–48 and 52–100 Hz) of 25 transitions of one rat of the G1 group (S1r–V1r, intrahemispheric coherence). (t) indicates the onset of REM sleep. (B) Waking from REM sleep. The graphs show the mean z' -coherence \pm standard deviation (for 30–48 and 52–100 Hz) of 25 transitions of one rat of the G1 group (S1r–V1r, intrahemispheric coherence). (t) indicates the end of the REM sleep episodes. NREM episodes are symbolized in green; REM episodes in red. The states that followed the REM sleep episodes are indicated in black (these epochs were mainly wakefulness but NREM sleep episodes also followed REM sleep). (For interpretation of the references to color in this figure legend, the reader is referred to the web version of this article.)

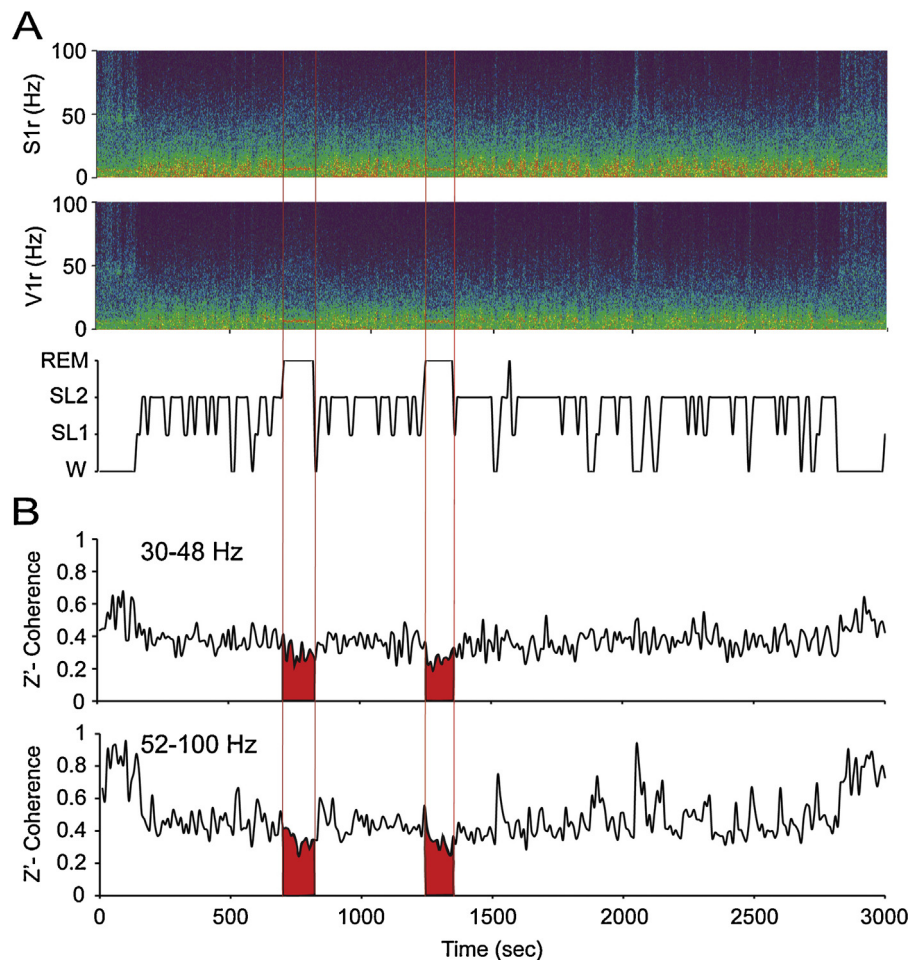


Fig. 6. Dynamic of the gamma coherence during wakefulness and sleep. (A) The spectrogram (0.1–100 Hz) of primary visual (V1r) and primary somatosensory (S1r) cortical recordings and the accompanying hypnogram are shown. During W and REM sleep the theta activity (4–9 Hz) in the spectrograms can be readily observed. Gamma activity is larger during W. During NREM sleep, delta activity (0.5–4 Hz) is more prominent and there are intermittent episodes of sigma activity (9–15 Hz), which correspond to the presence of sleep spindles. (B) The z' -coherence for both gamma bands (30–48 and 52–100 Hz) was analyzed in 10-s epochs. The maximum values of z' -coherence occurred during W; z' -coherence decreased to an intermediate level during NREM sleep and minimum values were present during the periods of REM sleep (segments in red). (For interpretation of the references to color in this figure legend, the reader is referred to the web version of this article.)

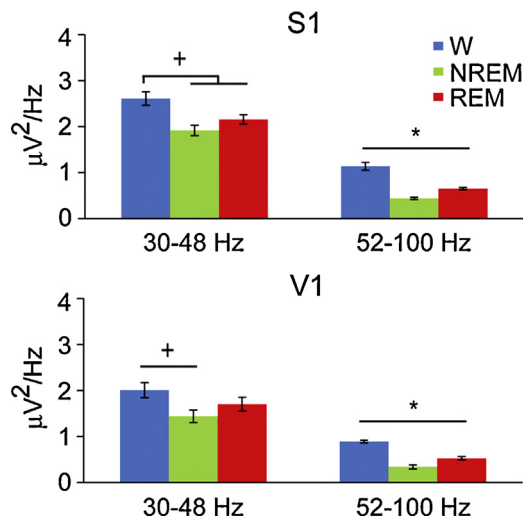


Fig. 7. Gamma power during wakefulness and sleep. Mean gamma band power of the EEG recorded from 3 rats of the intra-hemispheric S1r and V1r cortices of group G1 (see Fig. 1) during wakefulness (W), NREM and REM sleep. The values represent mean \pm standard error. Statistical significance: * $P < 0.05$ and ** $P < 0.0001$, ANOVA with Tamhane tests.

3.3. Gamma power during wakefulness and sleep

The gamma power was different across behavioral states for S1 (30–48 Hz, $F_{2,105} = 7.941$, $p = 0.001$; 52–100 Hz, $F_{2,105} = 49.37$, $p < 0.0001$) and V1 cortices (30–48 Hz, $F_{2,105} = 6.092$, $p = 0.003$; 52–100 Hz, $F_{2,105} = 45.06$, $p < 0.0001$). Fig. 7 shows that gamma power was significantly greater during W than during REM sleep for 52–100 Hz in S1 and V1 cortices, and for 30–48 Hz in S1 cortex. However, in contrast to z' -coherence values, the minimum power values occurred during NREM sleep.

4. Discussion

In the present study, we demonstrated in rats that the EEG intra-hemispheric and interhemispheric coherence in the gamma (30–48 and 52–100 Hz) frequency band is smaller during REM sleep than during W or NREM sleep. Therefore, these data suggest that during REM sleep, high-frequency functional interaction between different cortical regions is lower compared with other behavioral states.

4.1. Gamma coherence during wakefulness

It is well established that gamma power and gamma coherence increase during W in cats and humans, mainly for intrahemispheric combination of electrodes [4,6,7]. In the cat, gamma band coherence at ≈ 40 Hz increases during alert W; this fact that can be clearly observed in raw recordings [6,7]. In the present study, the largest gamma power and intrahemispheric coherence was present during W states, but the differences depending on waking conditions were not studied. In this regards, Maloney et al. (1998) showed that the largest values of gamma power occur during periods of active W [22].

4.2. Gamma coherence during REM sleep

In the present report, we demonstrated in rats that gamma intra and interhemispheric coherence reaches a nadir during REM sleep. This result accords with the results of our previous studies in the cat [6,7], where gamma coherence was almost absent during REM sleep in intrahemispheric and interhemispheric derivatives. The demonstration that there is a radical reduction in gamma

coherence between different cortical regions during REM sleep does not contradict the findings of Steriade et al. (1996), which showed an increase in local coupling (within a column or among closely cortical sites) during activated states [23]. In fact, as shown in Fig. 7, gamma power (as a reflection of local gamma synchronization) during REM sleep was close to W, and larger than during NREM sleep. Therefore, although gamma activity was large during REM sleep, the coupling of gamma oscillations between different cortical areas (reflected by gamma coherence) was minimal.

In humans, an early report showed that during REM sleep magneto-EEG 40-Hz oscillations were similar in distribution, phase and amplitude to those observed during W. In contrast, Perez-Garci et al. (2001) reported that there is a decrease in correlation spectra in 2-s epochs of fast (27–48 Hz) frequencies restricted to intra-hemispheric frontal-perceptual cortical regions during REM sleep. On the contrary, the gamma synchrony between homologous cortical regions of both hemispheres increases during REM sleep in humans [24,25]. Cantero et al. (2004) employed human intracranial EEG recordings for coherence analyses during sleep, which allowed a much finer spatial scale than scalp-recorded signals. They found that local (within neocortical regions) and long-range (between intra-hemispheric neocortical regions) gamma (35–58 Hz) coherence was significantly greater during wakefulness than during sleep. However, no differences in coherence were found between NREM and REM sleep. Furthermore, functional gamma-range coupling between the neocortex and hippocampus was observed during wakefulness, but not during REM sleep. Finally, Voss et al. (2009) demonstrated that gamma coherence decreases during REM sleep compared with wakefulness; during lucid dreaming, coherence values are intermediate between W and REM sleep.

As with other EEG rhythms, gamma oscillations remains remarkable conserved in mammals irrespective of brain size [26]. The decrease in gamma coherence during REM sleep in rats (present report), in cats [6,7] and in humans [24,27,28], indicates that during this behavioral state there is a decrease in the capacity for integration among different cortices within high frequency ranges.

A recent study demonstrated that electrical stimulation of the prefrontal cortex in the lower gamma band (≈ 40 Hz) during REM sleep influences ongoing brain activity and induces self-reflective awareness (a feature of W) in dreams (i.e., lucid dreams), while other stimulation frequencies were not effective [29]. Thus, the data support the concept that synchronous oscillations of ≈ 40 Hz are an electrophysiological pattern of activity that is indicative of attentive wakefulness. On the contrary, the reduction of gamma coherence during REM sleep [6,7,24,27,28], may underlie the unique pattern of REM sleep mentation, i.e., dreams [14,30].

5. Conclusions

During REM sleep in the rat, despite an activated EEG, there is an uncoupling of the gamma frequency activities between neocortical sites. Therefore, functional interactions among different cortical areas, which are critical for cognitive functions, are different during W and REM sleep. Since this feature is conserved in other mammals, including humans, we consider that this uncoupling of gamma frequency activity during REM sleep is a defining trait of REM sleep in mammals.

Acknowledgments

We are grateful to Dr. Horacio Igarzabal for his assistance in the experimental procedures. This study was partially supported by the “Programa de Desarrollo de Ciencias Básicas” (PEDECIBA) and the “Agencia Nacional de Investigación e Innovación” (ANII), Uruguay.

References

- [1] Rieder MK, Rahm B, Williams JD, Kaiser J. Human gamma-band activity and behavior. *Int J Psychophysiol* 2010;79:39–48.
- [2] Uhlhaas PJ, Pipa G, Lima B, Melloni L, Neuenschwander S, Nikolic D, et al. Neural synchrony in cortical networks: history, concept and current status. *Front Integr Neurosci* 2009;3:17.
- [3] Uhlhaas PJ, Pipa G, Neuenschwander S, Wibral M, Singer W. A new look at gamma? High- (>60 Hz) gamma-band activity in cortical networks: function, mechanisms and impairment. *Prog Biophys Mol Biol* 2011;105:14–28.
- [4] Llinas R, Ribary U. Coherent 40-Hz oscillation characterizes dream state in humans. *Proc Natl Acad Sci U S A* 1993;90:2078–81.
- [5] Tiitinen H, Sinkkonen J, Reinikainen K, Alho K, Lavikainen J, Naatanen R. Selective attention enhances the auditory 40-Hz transient response in humans. *Nature* 1993;364:59–60.
- [6] Castro S, Falconi A, Chase MH, Tortorolo P. Coherent neocortical 40-Hz oscillations are not present during REM sleep. *Eur J Neurosci* 2013;37:1330–9.
- [7] Castro S, Cavelli M, Vollono P, Chase MH, Falconi A, Tortorolo P. Inter-hemispheric coherence of neocortical gamma oscillations during sleep and wakefulness. *Neurosci Lett* 2014;578:197–202.
- [8] Bullock TH, McClune MC, Enright JT. Are the electroencephalograms mainly rhythmic? Assessment of periodicity in wide-band time series. *Neuroscience* 2003;121:233–52.
- [9] Edelman GM, Tononi G. A universe of consciousness. New York: Basic Books; 2000.
- [10] Siegel M, Donner TH, Engel AK. Spectral fingerprints of large-scale neuronal interactions. *Nat Rev Neurosci* 2012;13:121–34.
- [11] Llinas R, Ribary U, Contreras D, Pedraza C. The neuronal basis for consciousness. *Philos Trans R Soc Lond B: Biol Sci* 1998;353:1841–9.
- [12] John ER. The neurophysics of consciousness. *Brain Res Brain Res Rev* 2002;39:1–28.
- [13] Mashour GA. Integrating the science of consciousness and anesthesia. *Anesth Analg* 2006;103:975–82.
- [14] Hobson JA. REM sleep and dreaming: towards a theory of protoconsciousness. *Nat Rev Neurosci* 2009;10:803–13.
- [15] Benedetto L, Rodriguez-Servetti Z, Lagos P, D'Almeida V, Monti JM, Tortorolo P. Microinjection of melanin concentrating hormone into the lateral preoptic area promotes non-REM sleep in the rat. *Peptides* 2013;39C:11–5.
- [16] Lagos P, Tortorolo P, Jantos H, Chase MH, Monti JM. Effects on sleep of melanin-concentrating hormone microinjections into the dorsal raphe nucleus. *Brain Res* 2009;1265:103–10.
- [17] Bullock TH, Buzsaki G, McClune MC. Coherence of compound field potentials reveals discontinuities in the CA1-subiculum of the hippocampus in freely-moving rats. *Neuroscience* 1990;38:609–19.
- [18] Bullock TH. Signals and signs in the nervous system: the dynamic anatomy of electrical activity is probably information-rich. *Proc Natl Acad Sci U S A* 1997;94:1–6.
- [19] Bullock TH, McClune MC, Achimowicz JZ, Iragui-Madoz VJ, Duckrow RB, Spencer SS. EEG coherence has structure in the millimeter domain: subdural and hippocampal recordings from epileptic patients. *Electroencephalogr Clin Neurophysiol* 1995;95:161–77.
- [20] Cantero JL, Atienza M, Salas RM. Clinical value of EEG coherence as electrophysiological index of cortico-cortical connections during sleep. *Rev Neurol* 2000;31:442–54.
- [21] Nunez PL, Srinivasan R, Westdorp AF, Wijesinghe RS, Tucker DM, Silberstein RB, et al. EEG coherency. I: Statistics, reference electrode, volume conduction, Laplacians, cortical imaging, and interpretation at multiple scales. *Electroencephalogr Clin Neurophysiol* 1997;103:499–515.
- [22] Maloney KJ, Cape EG, Gotman J, Jones BE. High-frequency gamma electroencephalogram activity in association with sleep-wake states and spontaneous behaviors in the rat. *Neuroscience* 1997;76:541–55.
- [23] Steriade M, Amzica F, Contreras D. Synchronization of fast (30–40 Hz) spontaneous cortical rhythms during brain activation. *J Neurosci* 1996;16:392–417.
- [24] Perez-Garci E, del-Rio-Portilla Y, Guevara MA, Arce C, Corsi-Cabrera M. Paradoxical sleep is characterized by uncoupled gamma activity between frontal and perceptual cortical regions. *Sleep* 2001;24:118–26.
- [25] Corsi-Cabrera M, Sifuentes-Ortega R, Rosales-Lagarde A, Rojas-Ramos OA, Del Rio-Portilla Y. Enhanced synchronization of gamma activity between frontal lobes during REM sleep as a function of REM sleep deprivation in man. *Exp Brain Res* 2014;232:1497–508.
- [26] Buzsaki G, Logothetis N, Singer W. Scaling brain size, keeping timing: evolutionary preservation of brain rhythms. *Neuron* 2013;80:751–64.
- [27] Cantero JL, Atienza M, Madsen JR, Stickgold R. Gamma EEG dynamics in neocortex and hippocampus during human wakefulness and sleep. *Neuroimage* 2004;22:1271–80.
- [28] Voss U, Holzmann R, Tuin I, Hobson JA. Lucid dreaming: a state of consciousness with features of both waking and non-lucid dreaming. *Sleep* 2009;32:1191–200.
- [29] Voss U, Holzmann R, Hobson A, Paulus W, Koppehele-Gossel J, Klimke A, et al. Induction of self awareness in dreams through frontal low current stimulation of gamma activity. *Nat Neurosci* 2014;17:810–2.
- [30] Nir Y, Tononi G. Dreaming and the brain: from phenomenology to neurophysiology. *Trends Cogn Sci* 2010;14:88–100.
- [31] Paxinos G, Watson C. The rat brain. New York: Academic Press; 2005.